

## Role of step-flow advection during electromigration-induced step bunching

Matthieu Dufay,<sup>1</sup> Thomas Frisch,<sup>2</sup> and Jean-Marc Debierre<sup>1</sup>

<sup>1</sup>Laboratoire Matériaux et Microélectronique de Provence, Aix-Marseille Université and CNRS, Faculté des Sciences et Techniques de Saint-Jérôme, Case 151, 13397 Marseille Cedex 20, France  
<sup>2</sup>Institut de Recherche sur les Phénomènes Hors Equilibre, Aix-Marseille Université, Ecole Centrale Marseille and CNRS, 49, rue Joliot Curie, Boîte Postale 146, 13384 Marseille Cedex 13, France

(Received 1 June 2007; published 21 June 2007)

We propose a one-dimensional model based on the Burton-Cabrera-Frank equations to describe the electromigration-induced step bunching instability on vicinal surfaces. The step drift resulting from atomic evaporation and/or deposition is explicitly included in our model. A linear stability analysis reveals several stability inversions as the evaporation rate varies, while a deposition flux is shown to have a stabilizing effect.

DOI: 10.1103/PhysRevB.75.241304

PACS number(s): 66.30.Qa, 05.70.Ln, 81.15.Aa

Due to its importance for both fundamental science and technological applications in microelectronics, research in the field of crystal growth on semiconductor vicinal surfaces has become increasingly active.<sup>1-6</sup> Vicinal surfaces are slightly misoriented with respect to closed-packed crystalline planes of low indices, such as the well-studied Si(111) plane. The atomic steps resulting from the miscut are generally mobile (step flow) and subject to a number of instabilities as step bunching or meandering.<sup>3,7-11</sup> At long times, nonlinear dynamics lead to the formation of more or less well-organized surface patterns. The idea to control these patterns is appealing, a major issue being the self-organization of nanostructures on semiconductor surfaces. A few ways to reach this goal are currently under investigation, such as imposing a net atomic flux (evaporation or deposition), using elastic stresses, or applying a constant electrical field inducing an adatom drift (surface electromigration). Combinations of these methods allow extra flexibility.<sup>6,12</sup> Surface electromigration was first observed by Latyshev *et al.*,<sup>13</sup> and an early theory proposed by Stoyanov.<sup>14</sup> The stability of a Si(111) vicinal surface may change according to the temperature, the sign of the net atomic flux, and the direction of the electrical current. Three temperature regimes have been identified experimentally.<sup>15-18</sup> Both in the high- and low-temperature regimes, the step bunching instability appears when the electrical current is applied in the step-down direction. Alternatively, in the intermediate regime, it may be necessary (according to the experimental conditions) to apply a step-up current to trigger step bunching. This stability inversion with respect to the direction of the electrical current is still the subject of active research and different mechanisms have been proposed such as sign variations of the effective charge number ( $Z^*$ ) with temperature, step transparency,<sup>19,20</sup> and two-region terrace diffusion.<sup>21</sup> While sign variations of  $Z^*$  with temperature have been ruled out by a recent experiment of mass transport across a trench,<sup>22</sup> the two other possibilities remain. However, due to the large number of experimental parameters and ultrahigh vacuum conditions, direct *in situ* experimental measurements of adatom diffusion at the step edges are still difficult to achieve. In this Rapid Communication, we propose a one-dimensional model based on the Burton-Cabrera-Frank equations<sup>23</sup> to describe the step flow instabilities arising when electromigration is combined

with a net atomic flux. We first remark that, under typical experimental conditions, the advection effects due to the mean step velocity are comparable in magnitude with the drift due to the electromigration current. Both effects are thus included in our model and a linear stability analysis shows that the interplay between them does provoke stability inversions as evaporation is increased.

During evaporation or growth, the steps of Si(111) vicinal surfaces undergo a global drift with a constant mean velocity  $V_0$ . In the frame moving at this velocity, the adatom concentration  $C_n$  on the  $n$ th terrace obeys the following quasistatic equation:

$$D_s \partial_{XX} C_n + \left( V_0 - \frac{D_s}{\ell_E} \right) \partial_X C_n - \frac{C_n}{\tau} + F = 0, \quad (1)$$

where  $D_s$  is the diffusion coefficient,  $\ell_E = k_B T / (Z^* e E)$  is the electrical length,  $\tau$  is the desorption time, and  $F$  is the atomic deposition flux. As shown in Fig. 1, the electrical field reads  $\mathbf{E} = E \hat{\mathbf{X}}$ , with  $\hat{\mathbf{X}}$  the unit vector pointing in the step-down direction. At terrace ends  $X = X_n$  and  $X = X_{n+1}$ , Eq. (1) is subject to the following boundary conditions:

$$(D_s \partial_X + V_0 - D_s / \ell_E) C_n = \nu [C_n - C_n^{eq}], \quad (2)$$

$$(D_s \partial_X + V_0 - D_s / \ell_E) C_n = -\nu [C_n - C_{n+1}^{eq}], \quad (3)$$

which ensure mass conservation. Here  $\nu$  is the step kinetic coefficient,  $C_n^{eq}$  is the adatom equilibrium concentration at step  $n$ , and we neglect step transparency. We can remark from the structure of Eqs. (1)–(3) that the advection and the electromigration terms play a similar role. The associated velocities  $V_0$  and  $D_s / \ell_E$  may be both positive or negative,

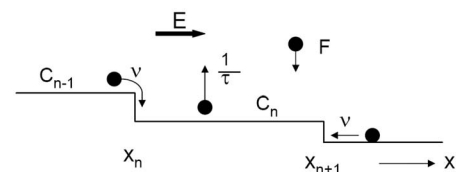


FIG. 1. Schematic side view of a vicinal surface: notations and definitions. The electrical field is imposed in the step-down direction here.

according to the sign of the imposed net atomic flux and electrical current. The advection terms are usually neglected in theoretical studies, which is equivalent to setting  $V_0$  to zero in Eqs. (1)–(3). However, on the basis of the present experimental knowledge, it seems unrealistic to neglect advection as compared to electromigration. On one hand, the net atomic flux varies in a rather wide range in practice (three decades) while the mean terrace width extends over one decade at least. As a consequence, the corresponding values of the mean step velocity  $V_0$  typically range from  $10^{-10}$  to  $10^{-6}$  m s $^{-1}$ . On the other hand, due to the experimental uncertainties on the values of the effective charge number  $Z^*$  and, to a less extent, to the temperature influence on the adatom diffusion coefficient  $D_s$ , estimates of the drift velocity  $D_s/\ell_E$  are found to lie in the very same range. Except in equilibrium conditions, the two effects are thus similar both in nature and in magnitude, so that we will keep the  $V_0$  terms in our model. At a given time  $t$ , the velocity of step  $n$  is  $V_n = \Omega_s \nu [C_n + C_{n-1} - 2C_n^{eq}] - V_0$ , where the concentrations are evaluated at  $X = X_n(t)$ , and  $\Omega_s$  represents the unit atomic surface. The terrace lengths  $L_n(t) = X_{n+1}(t) - X_n(t)$  vary slowly in time, with a constant mean value  $L_0$ . We introduce standard step-step repulsive interactions in the adatom equilibrium concentration,  $C_n^{eq}/C_0 = 1 + A(1/L_n^3 - 1/L_{n-1}^3)$ , where  $k_B T A \Omega_s^{-1}$  is the step-step interaction coefficient.<sup>24</sup> Setting the unit length to the initial terrace width  $L_0$  and the unit time to  $t_0 = L_0^2/D_s$ , we define the dimensionless variables  $x = X/L_0$ ,  $v_0 = V_0 t_0/L_0$ ,  $c_n = C_n/C_0$ , and  $c_n^{eq} = C_n^{eq}/C_0$ . For these variables, the previous equations become

$$(\partial_x + v_0 - \eta) \partial_x c_n - s^2 c_n + f = 0, \quad x_n < x < x_{n+1}, \quad (4)$$

$$(\partial_x + v_0 - \eta) c_n = \rho(c_n - c_n^{eq}), \quad x = x_n, \quad (5)$$

$$(\partial_x + v_0 - \eta) c_n = -\rho(c_n - c_{n+1}^{eq}), \quad x = x_{n+1}, \quad (6)$$

$$v_n = \phi \rho(c_n + c_{n-1} - 2c_n^{eq}) - v_0, \quad x = x_n, \quad (7)$$

with  $c_n^{eq} = 1 + a(1/l_n^3 - 1/l_{n-1}^3)$ . The system dynamics is thus controlled by six independent nondimensional parameters:  $\eta = L_0/\ell_E$  is proportional to the electrical field,  $s^2 = L_0^2/(D_s \tau)$  involves the rate of desorption and  $f = FL_0^2/(D_s C_0)$  is the atomic deposition flux,  $\rho = \nu L_0/D_s$  compares attachment to diffusion,  $\phi = \Omega_s C_0$  gives the proportion of occupied sites, and  $a = A/L_0^3$  measures step-step repulsion. These six parameters are not completely independent in practice. As a consequence, when temperature is varied in a given experimental setup, the system is driven along a rather complex trajectory in the parameter space. This trajectory is very likely to cross a succession of stable and unstable regions, as often observed in practice.

To provide quantitative support to this idea, we now perform the linear stability analysis of a uniform train of steps traveling at a constant velocity  $v_0$  in the laboratory frame. Let us remark that we keep the notation  $t$  for the dimensionless time hereafter. A general solution of Eq. (4) giving the concentration profile on terrace  $n$  is  $c_n = f/s^2 + \alpha_n e^{r_1 x} + \beta_n e^{r_2 x}$ , where  $r_{1,2} = -(v_0 - \eta)/2 \pm 1/2[(v_0 - \eta)^2 + 4s^2]^{1/2}$ . To avoid lengthy expressions, we first set  $f=0$  and we discuss the case

$f > 0$  later on. For the unperturbed system, we find that  $v_0$  obeys the following transcendental equation:

$$\frac{v_0}{\phi \rho} = \frac{2s^2(u_1 - u_2) - \rho u_1 u_2 \Lambda}{d_1 - d_2}, \quad (8)$$

where  $\Lambda = r_1 - r_2$ ,  $u_1 = e^{r_1} - 1$ ,  $u_2 = e^{r_2} - 1$ ,  $d_1 = (r_1 + \rho)(r_2 - \rho)e^{r_1}$ , and  $d_2 = (r_1 - \rho)(r_2 + \rho)e^{r_2}$ . We give an approximate expression for  $v_0$  in Eq. (11). The linear stability of the system is tested by adding a small harmonic perturbation of wave number  $k$ , on the step positions,  $x_n = n + \epsilon e^{ikn + \xi t}$ . In order to find the dispersion relation  $\xi = \sigma + i\omega$ , we expand the step velocities up to the first order in the perturbation amplitude,  $\epsilon \ll 1$ . We obtain the following exact expression for the growth rate:

$$\sigma(k) = 2\phi \rho \sin^2\left(\frac{k}{2}\right) \frac{A_1 s^2 + a(A_2 + A_3 \cos k)}{s^2(d_1 - d_2)^2}, \quad (9)$$

where

$$\frac{A_1}{\Lambda \rho} = [r_1 d_2 - r_2 d_1 + 2\rho \Lambda(r_1 + r_2)] e^{r_1 + r_2} + r_2 d_2 - r_1 d_1,$$

$$A_2 = 6s^2(d_2 - d_1)[2s^2(u_2 - u_1) - \rho \Lambda(u_1 + u_2 + 2)],$$

$$A_3 = 6s^2 \rho \Lambda (d_2 - d_1)(1 + e^{r_1 + r_2}). \quad (10)$$

In the parameter space, this allows us to compute the critical values of the parameters defining the boundaries between stable and unstable regions. One thus has to solve the system of two equations, Eqs. (8) and (9), in the two unknowns,  $\eta$  and  $v_0$ . Remarking that the condition  $|v_0 - \eta| \ll s$  is always verified for the practical values of the electrical field and net atomic flux, we obtain analytical expressions for the velocity,

$$v_0 = -2\phi \rho s \frac{e^s - 1}{\rho(1 + e^s) + s(e^s - 1)}, \quad (11)$$

and the growth rate,

$$\frac{\sigma(k)}{4\phi \rho} = \sin^2\left(\frac{k}{2}\right) \frac{B_1(v_0 - \eta) + a(B_2 + B_3 \cos k)}{s d_3^2}, \quad (12)$$

with  $d_3 = (s + \rho)^2 e^{2s} - (s - \rho)^2$ , and

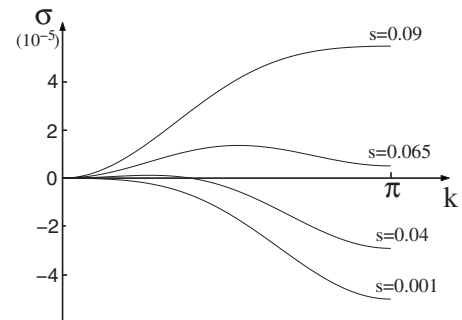


FIG. 2. Growth rate  $\sigma$  as a function of the wave number  $k$ , as obtained from Eqs. (12) and (13). Different evaporation rates  $s$  are considered. Nondimensional parameters are  $\phi=0.2$ ,  $f=0$ ,  $\eta=-10^{-4}$ ,  $\rho=20.0$ ,  $a=5 \times 10^{-6}$ .

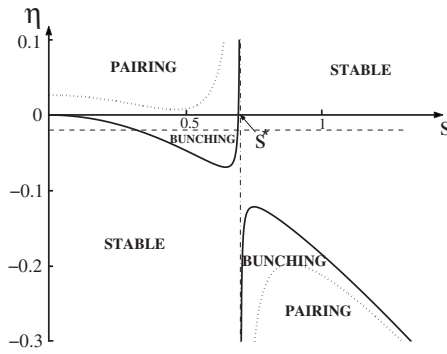


FIG. 3. Stability diagram in the  $(s, \eta)$  plane. Solid (dotted) curves represent  $\eta_c$  ( $\eta_p$ ). Nondimensional parameters are  $\phi=0.2$ ,  $f=0$ ,  $\rho=20.0$ ,  $a=10^{-4}$ . For a step-up electrical field, the horizontal dashed line represents a trajectory as the evaporation rate increases.

$$\frac{B_1}{\rho s^2 e^s} = (s + \rho)^2 (s - 1) e^{2s} - 4\rho s e^s + (s - \rho)^2 (s + 1),$$

$$B_2 = -6s^2 d_3 [(s + \rho) e^{2s} + \rho - s], \quad B_3 = 12s^2 d_3 \rho e^s. \quad (13)$$

Depending on the physical parameters, the growth rate  $\sigma(k)$  assumes negative or positive values. In the latter case, the one-dimensional train of steps is linearly unstable. The variations of the growth rate with the perturbation wave number  $k$  are displayed in Fig. 2 for different values of the evaporation parameter  $s$ . The electrical field is imposed in the step-up direction here ( $\eta < 0$ ). For  $s=0.001$  all the modes are stable, while the large wavelengths are unstable for  $s=0.04$ . At higher evaporation rates, all the wave numbers are unstable. Note that for  $s=0.09$ , the most unstable mode is obtained for  $k=\pi$  (step-pairing instability). Using Eqs. (11)–(13), we obtain the analytical expression for the boundary lines  $\eta_c(s)$  separating the stable and the step bunching regions in the  $(s, \eta)$  plane:

$$\eta_c = v_0 + \left( \frac{B_2 + B_3}{B_1} \right) a. \quad (14)$$

In addition, one shows that step-pairing instability becomes the most unstable mode for  $\eta_p = v_0 + a(B_2 - 3B_3)/B_1$ .

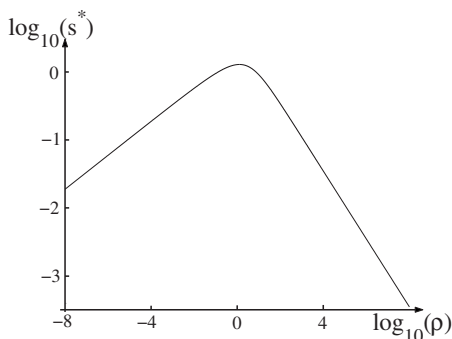


FIG. 4. Critical value of the nondimensional evaporation rate  $s^*$  as a function of the attachment vs diffusion parameter  $\rho$  for  $f=0$  (log-log scales).

The stability diagram representing the boundaries between the stable and unstable regions is shown in Fig. 3. For typical values of the step-up electrical field (500 V/m),  $\eta$  assumes small negative values (lower than  $10^{-2}$  in magnitude) which lie slightly below the horizontal axis in the  $(s, \eta)$  plane.<sup>28</sup> Since the evaporation rate  $s$  becomes larger as temperature is increased, the system is stable both at low and high temperatures and it becomes unstable in the intermediate temperature range. Indeed, this succession of stability reversals is observed experimentally for step-up currents.<sup>15–18</sup> In the unstable regions, both for step-up and step-down currents, step bunching is superseded by the step-pairing instability for large electrical fields. Moreover, the bunching regions progressively reduce in size as the step-step interaction coefficient  $a$  is decreased. As shown by Eqs. (13) and (14), the location of the vertical asymptote  $s=s^*$  solely varies with the attachment vs diffusion parameter  $\rho$ . These variations are represented in Fig. 4. A maximum is obtained for  $\rho \approx 1$ , when the attachment length  $d=D_s/\nu$  is comparable to the terrace width  $L_0$ . For attachment-limited dynamics,  $\rho < 1$ , we find that  $s^* \approx (12\rho)^{1/4}$ , while  $s^* \approx (12/\rho)^{1/2}$  for diffusion-limited dynamics,  $\rho > 1$ . As discussed above,  $|\eta| < 10^{-2}$  in practice, so that the highest critical value of the evaporation rate is very close to  $s=s^*$ . Since the desorption time reads  $\tau=L_0^2/(s^2 D_s)$ , we respectively obtain  $\tau^*=(L_0^3/12\nu D_s)^{1/2}$ , and  $\tau^*=\nu L_0^3/12D_s^2$  in the attachment-limited and the diffusion-limited regimes. This implies that  $s^*$  strongly depends on the miscut angle.

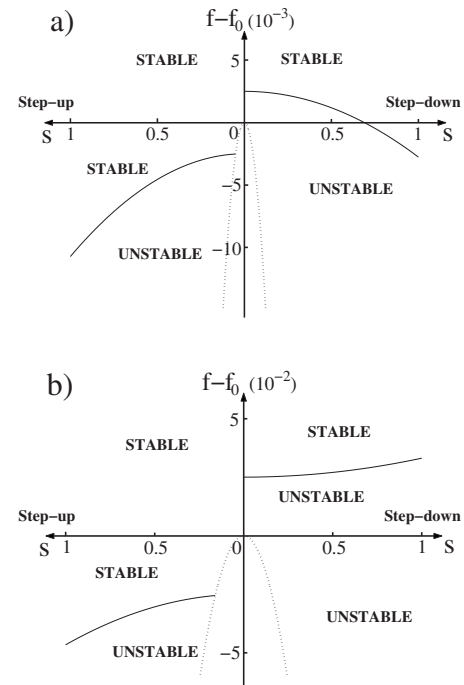


FIG. 5. Stability diagrams in the  $(s, f-f_0)$  plane. Horizontal axes  $f=f_0$  correspond to zero net flux. On the left (right) side of the vertical axes, the electrical current is step-up (step-down). Solid lines represent the boundaries between stable and unstable regions. The regions below the dotted lines are unphysical ( $f < 0$ ). Nondimensional parameters are  $\phi=0.2$ ,  $\rho=1.0$ ,  $a=10^{-4}$ , and we set (a)  $\eta = \pm 5.0 \times 10^{-4}$ , (b)  $\eta = \pm 5.0 \times 10^{-3}$ .

Let us discuss now the case of a nonzero deposition flux,  $f > 0$ . The drift velocity reads

$$v_0 = -2\phi\rho \frac{(s^2 - f)(e^s - 1)}{s\rho(1 + e^s) + s^2(e^s - 1)}. \quad (15)$$

It vanishes when the deposition and evaporation fluxes compensate,  $f = f_0 = s^2$ . We first consider the case of a step-up current. The step bunching instability occurs only when evaporation dominates deposition,  $f < f_0$ , as shown on the left side of Fig. 5. On the other hand, for a step-down current, the instability may occur both for  $f < f_0$  and  $f > f_0$ , depending on the values of the physical parameters. From Fig. 5, it is also clear that increasing the deposition flux has a stabilizing effect, whatever the direction of the electrical field. Since  $a \sim L_0^{-3}$ , after Eq. (14) the stability threshold

$\eta_c \simeq v_0$  for large  $L_0$  values. Thus measurements of the step velocity  $V_0$  could provide direct estimates of the effective charge number,  $Z^* = (V_0 k_B T) / (D_s e E)$ .

In conclusion, we have shown that advection cannot in general be neglected as compared to electromigration. We have identified a set of six nondimensional parameters governing the system evolution. For step-up electrical currents, two stability inversions have been found as evaporation increases. Numerical simulations of our model equations are currently performed to investigate nonlinear regimes, such as coarsening dynamics, oscillating modes and spatiotemporal chaos.<sup>25-27</sup>

It is a pleasure to thank F. Leroy, J.-J. Métois, P. Müller, O. Pierre-Louis, and A. Verga for fruitful discussions.

- 
- <sup>1</sup>Y. Saito, *Statistical Physics of Crystal Growth* (World Scientific, Singapore, 1998).
- <sup>2</sup>A. Pimpinelli and J. Villain, *Physics of Crystal Growth* (Cambridge University Press, Cambridge, England, 1998).
- <sup>3</sup>H.-C. Jeong and E. D. Williams, *Surf. Sci. Rep.* **34**, 171 (1999).
- <sup>4</sup>P. Politi, G. Grenet, A. Marty, A. Ponchet, and J. Villain, *Phys. Rep.* **324**, 271 (2000).
- <sup>5</sup>K. Yagi, H. Minoda, and M. Degawa, *Surf. Sci. Rep.* **43**, 45 (2001).
- <sup>6</sup>J. Stangl, V. Holy, and G. Bauer, *Rev. Mod. Phys.* **76**, 725 (2004).
- <sup>7</sup>D.-J. Liu and J. D. Weeks, *Phys. Rev. B* **57**, 14891 (1998).
- <sup>8</sup>T. Frisch and A. Verga, *Phys. Rev. Lett.* **94**, 226102 (2005).
- <sup>9</sup>M. Sato, M. Uwaha, and Y. Saito, *Phys. Rev. B* **72**, 045401 (2005).
- <sup>10</sup>O. Pierre-Louis, *Phys. Rev. Lett.* **96**, 135901 (2006).
- <sup>11</sup>M. Dufay, J. M. Debiere, and T. Frisch, *Phys. Rev. B* **75**, 045413 (2007).
- <sup>12</sup>O. Fruchart, *C. R. Phys.* **6**, 1 (2005).
- <sup>13</sup>A. V. Latyshev, A. L. Aseev, A. B. Krasilnikov, and S. I. Stenin, *Surf. Sci.* **213**, 157 (1989).
- <sup>14</sup>S. Stoyanov, *Jpn. J. Appl. Phys., Part 1* **30**, 1 (1991).
- <sup>15</sup>J. J. Métois and S. Stoyanov, *Surf. Sci.* **440**, 407 (1999).
- <sup>16</sup>K. Fujita, M. Ichikawa, and S. S. Stoyanov, *Phys. Rev. B* **60**, 16006 (1999).
- <sup>17</sup>B. J. Gibbons, J. Noffsinger, and J. P. Pelz, *Surf. Sci.* **575**, L51 (2005).
- <sup>18</sup>B. J. Gibbons, S. Schaepe, and J. P. Pelz, *Surf. Sci.* **600**, 2417 (2006).
- <sup>19</sup>O. Pierre-Louis, *Surf. Sci.* **529**, 114 (2003).
- <sup>20</sup>O. Pierre-Louis and J.-J. Métois, *Phys. Rev. Lett.* **93**, 165901 (2004).
- <sup>21</sup>T. Zhao, J. D. Weeks, and D. Kandel, *Phys. Rev. B* **70**, 161303(R) (2004).
- <sup>22</sup>M. Degawa, H. Minoda, Y. Tanishiro, and K. Yagi, *Surf. Sci. Lett.* **461**, L528 (2000).
- <sup>23</sup>W. K. Burton, N. Cabrera, and F. C. Frank, *Philos. Trans. R. Soc. London, Ser. A* **243**, 299 (1951).
- <sup>24</sup>P. Müller and A. Saúl, *Surf. Sci. Rep.* **54**, 593 (2004).
- <sup>25</sup>J. Krug, V. Tonchev, S. Stoyanov, and A. Pimpinelli, *Phys. Rev. B* **71**, 045412 (2005).
- <sup>26</sup>V. Popkov and J. Krug, *Phys. Rev. B* **73**, 235430 (2006).
- <sup>27</sup>J. Chang, O. Pierre-Louis, and C. Misbah, *Phys. Rev. Lett.* **96**, 195901 (2006).
- <sup>28</sup>Under typical experimental conditions on a Si(111) surface,  $E = 400 - 700 \text{ V m}^{-1}$ ,  $L_0 = 10^{-9} - 10^{-5} \text{ m}$ ,  $A = 10^{-28} - 10^{-26} \text{ m}^3$ ,  $T = 1200 - 1650 \text{ K}$ ,  $Z^* = 10^{-3} - 10^{-1}$ ,  $C_0 \Omega_s = 0.2$ ,  $\tau = \tau_0 \exp(E_{des}/k_b T)$ , with  $\tau_0 = 10^{-15} \text{ s}$ ,  $E_{des} = 4.2 \text{ eV}$ ,  $D_s = D_0 \exp(-E_d/k_b T)$ , with  $D_0 = 10^{-6} \text{ m}^2/\text{s}$ ,  $E_d = 1.1 \text{ eV}$ . We find, for instance,  $s = 10^{-4} - 10^0$  and  $\eta = 10^{-2} - 10^{-8}$ .